Title

Effects of intravitreal injection of human CD34+ bone marrow stem cells in a murine model of diabetic retinopathy

Authors

Yazdanyar, Amirfarbod

Zhang, Pengfei

Dolf, Christian

et al.

Publication Date

2020

DOI

10.1016/j.exer.2019.107865

Peer reviewed

HHS Public Access

Author manuscript

Exp Eye Res. Author manuscript; available in PMC 2021 January 01.

Published in final edited form as:

Exp Eye Res. 2020 January ; 190: 107865. doi:10.1016/j.exer.2019.107865.

Effects of Intravitreal Injection of Human CD34+ Bone Marrow Stem Cells in a Murine Model of Diabetic Retinopathy

Amirfarbod Yazdanyar, M.D., Ph.D.[1], **Pengfei Zhang, Ph.D.**[2], **Christian Dolf**[1], **Zeljka Smit-McBride, Ph.D.**[1,3], **Whitney Cary**[4], **Jan A. Nolta, Ph.D.**[4], **Robert J. Zawadzki, Ph.D.**[1,2], **Nicholas Marsh-Armstrong, Ph.D.**[1], **Susanna S. Park, M.D., Ph.D.**[1]

[1]Department of Ophthalmology & Vision Science, University of California Davis Eye Center, Sacramento, California, United States

[2]Eye-POD Small Animal Ocular Imaging Laboratory, Department of Cell Biology and Human Anatomy, University of California, Davis, California, United States

[3]Vitreoretinal Research Laboratory, Department of Ophthalmology & Vision Science, University of California Davis, Davis, California, United States

[4]Stem Cell Program, Institute for Regenerative Cures, University of California Davis Medical Center, Sacramento, California, United States

Abstract

Human CD34+ stem cells are mobilized from bone marrow to sites of tissue ischemia and play an important role in tissue revascularization. This study used a murine model to test the hypothesis that intravitreal injection of human CD34+ stem cells harvested from bone marrow (BMSCs) can have protective effects in eyes with diabetic retinopathy. Streptozotocin-induced diabetic mice (C57BL/6J) were used as a model for diabetic retinopathy. Subcutaneous implantation of Alzet pump, loaded with Tacrolimus and Rapamycin, 5 days prior to intravitreal injection provided continuous systemic immunosuppression for the study duration to avoid rejection of human cells. Human CD34+ BMSCs were harvested from the mononuclear cell fraction of bone marrow from a healthy donor using magnetic beads. The CD34+ cells were labeled with enhanced green fluorescent protein (EGFP) using a lentiviral vector. The right eye of each mouse received an intravitreal injection of 50,000 EGFP-labeled CD34+ BMSCs or phosphate buffered saline (PBS). Simultaneous multimodal *in vivo* retinal imaging system consisting of fluorescent scanning laser ophthalmoscopy (enabling fluorescein angiography), optical coherence tomography (OCT) and OCT angiography was used to confirm the development of diabetic retinopathy and study the in vivo migration of the EGFP-labeled CD34+ BMSCs in the vitreous and retina following intravitreal injection. After imaging, the mice were euthanized, and the eyes were removed for

Corresponding Author: Susanna S. Park, MD., Ph.D., Department of Ophthalmology & Vision Science, University of California, Davis Eye Center, 4860 Y Street, Suite 2400, Sacramento, CA 95817 USA, Tel: 916-734-6074; FAX: 916-734-6197, sscpark@ucdavis.edu.

Commercial Relationships: Contracted research (Allergan, Roche/Novartis—SSP); no other relationship to disclose

immunohistochemistry. In addition, microarray analysis of the retina and retinal flat mount analysis of retinal vasculature were performed. The development of retinal microvascular changes consistent with diabetic retinopathy was visualized using fluorescein angiography and OCT angiography between 5 and 6 months after induction of diabetes in all diabetic mice. These retinal microvascular changes include areas of capillary nonperfusion and late leakage of fluorescein dye. Multimodal in vivo imaging and immunohistochemistry identified EGFP-labeled cells in the superficial retina and along retinal vasculature at 1 and 4 weeks following intravitreal cell injection. Microarray analysis showed changes in expression of 162 murine retinal genes following intravitreal CD34+ BMSC injection when compared to PBS-injected control. The major molecular pathways affected by intravitreal CD34+ BMSC injection in the murine retina included pathways implicated in the pathogenesis of diabetic retinopathy including Toll-like receptor, MAP kinase, oxidative stress, cellular development, assembly and organization pathways. At 4 weeks following intravitreal injection, retinal flat mount analysis showed preservation of the retinal vasculature in eyes injected with CD34+ BMSCs when compared to PBS-injected control. The study findings support the hypothesis that intravitreal injection of human CD34+ BMSCs results in retinal homing and integration of these human cells with preservation of the retinal vasculature in murine eyes with diabetic retinopathy.

Keywords

Bone marrow stem cells; CD34+ cells; cell therapy; diabetic retinopathy; intravitreal cell injection; microarray analysis; retinal imaging; optical coherence tomography; stem cells

1. INTRODUCTION

Diabetes mellitus is a major health issue worldwide and its incidence is projected to increase in the coming decades (Zheng et al., 2012). Diabetic retinopathy is the leading cause of blindness among working-aged adults worldwide (Kocur & Resnikoff, 2002). It is characterized by retinal vascular damage, leading to retinal ischemia, hemorrhage, exudation and complications such as retinal neovascularization and macular edema. Intravitreal drug therapy and retinal laser photocoagulation are available treatments to minimize vision loss associated with these complications. However, no treatment is available for vision loss resulting from retinal ischemia and/or retinal degeneration associated with diabetic retinopathy.

Various stem cells are being explored as regenerative treatment for retinal disorders in preclinical and early phase clinical studies (Park et al., 2017). They include pluripotent stem cells that are being explored for tissue replacement and adult stem cells in the bone marrow that are being explored for their known paracrine trophic effects. Much of the research using pluripotent stem cells have concentrated on subretinal administration of stem cells to treat degenerating outer retinal disorders. In the case of retinal vasculopathy, such as diabetic retinopathy, intravitreal administration of bone marrow stem cells (BMSCs) is a strategy that can be explored to repair the retinal vasculature and neurons in the inner retina.

Several different types of adult stem cells, harvested mostly from bone marrow, have been explored for neuroprotection in preclinical and clinical studies using various routes of

administration. Cultured mesenchymal stem cells have been explored in clinical trails showing safety and feasibility with intravenous administration in patients with diabetic retinopathy (Gu et al., 2018), but safety concerns were noted following intravitreal or subretinal administration despite potential neuroprotective effects (Ezquer et al., 2016; Oner et al., 2016; Park et al., 2016; Wang et al., 2017). More recently, intravitreal administration of murine CD133+ cells from bone marrow have been explored in a murine model of diabetic retinopathy showing potential neuroprotective effects (Rong et al., 2018). CD133 is a cell surface marker that has been used to identify human hematopoietic stem cells (HSCs).

Since diabetic retinopathy is characterized by chronic progressive retinal vascular damage as well as retinal neuro-degeneration, a safe cellular therapy that could protect the retinal vasculature as well as the retinal neurons would be of interest. Human bone marrow contains CD34+ stem cells, a subpopulation consisting of HSCs and endothelial progenitor cells. These cells play an important role in tissue repair and angiogenesis after ischemia.[3] Thus, they are ideal cells to explore as potential regenerative treatment for diabetic retinopathy. In clinical trials of cardiomyopathy, intracoronary infusion of autologous CD34+ or mononuclear cells (i.e. crude cell mixture containing some CD34+ cells) has shown efficacy that correlate with the amount of CD34+ cells administered (Frijak et al., 2018; Mackie & Losordo, 2011).

Preclinical studies to date show that intravitreal injection of human CD34+ cells is a feasible approach to deliver these cells to the damaged retinal vasculature in eyes with retinal vasculopathy (Caballero et al., 2007; Park et al., 2012). These human cells rapidly home into the damaged retinal vasculature following intravitreal injection and can be identified as late as 6 months after a single intravitreal administration. The potential protective effects of these human CD34+ cells on the retinal vasculature have not been clearly demonstrated in these animal models to date due to the transient nature of retinal vascular injury and/or limited systemic immunosuppression used to avoid rejection of human cells in prior studies.

Intravitreal injection of autologous CD34+ BMSCs has been explored in a phase 1 clinical trial showing safety and feasibility in eyes with retinal ischemia or degeneration (Park et al., 2015). Visual gain was noted in some treated eyes. This report did not include eyes with diabetic retinopathy. Before exploring efficacy of intravitreal CD34+ BMSCs as a potential treatment for diabetic retinopathy in a clinical trial, it would be important to determine if there are beneficial effects of these human CD34+ cells in eyes with diabetic retinopathy using animal models. In this study, a murine model of diabetic retinopathy with chronic systemic immunosuppression was used to determine whether intravitreal injection of human CD34+ BMSCs can have protective effects on the retina. Multimodal *in vivo* retinal imaging and immunohistochemistry were used to evaluate retinal homing and integration of these human CD34+ BMSCs. Microarray analysis of the murine retina was conducted to evaluate molecular changes in the retina associated with the CD34+ BMSC injection. Retinal flat mount immunohistochemistry was used to evaluate for changes in retinal vascular density.

2. MATERIALS AND METHODS

2.1 Animal Model

This study was conducted according to a protocol approved by the Institutional Animal Care and Use Committee at the University of California Davis and in accordance with the ARVO statement for the Use of Animals in Ophthalmic and Vision Research and NIH guidelines for care and use of animals in research. Male streptozotocin (STZ)-induced diabetic mice (C57BL/6J; Jackson Laboratories, Sacramento, CA, USA) were obtained commercially after confirmation of diabetes mellitus by Jackson's scientific staff. The protocol used by Jackson Laboratory to induce diabetes in C57Bl/6J mice is like that previously described with minor modifications (Feit-Letchman et al., 2005). Briefly, 6-week-old male C57BL/6J mice received 5 daily intraperitoneal injections of STZ (50mg/kg). When blood sugar was measured > 250 mg/dL on day 7, the development of diabetes was confirmed and the mice were shipped to the study center vivarium. The STZ-induced diabetic mice (n=40) were maintained in a high barrier, pathogen-free facility where all mice were monitored daily. Insulin was not administered for the course of the study. The diabetic mice maintained their weight during the course of the study but were smaller in size than age-matched non-diabetic mice. Polyurea was observed among diabetic mice requiring more frequent bedding changes. For control, wildtype age-matched non-diabetic C57BL/6J mice were also obtained commercially (n=10; Jackson Laboratories, Sacramento, CA, USA).

2.2 Immunosuppression

Systemic immunosuppression was started in all mice 5 days before intravitreal injection to prevent cross-species rejection of human cells. Immunosuppression was achieved by subcutaneous implantation of Alzet micro-osmotic pumps (model 1004; Durect Corporation, Cupertino, CA, USA) preloaded with immunosuppressive agents (Tacrolimus (FK506) and Rapamycin) as described previously (Moisseiev et al., 2016). This pump releases each drug at a constant rate of 1ug/g/day for up to 5 weeks after implantation.

2.3 CD34+ Cell Isolation and EGFP Labeling

Fresh human bone marrow from a healthy donor was purchased from StemExpress (Placerville, CA, USA). The CD34+ cells were harvested from the mononuclear cell fraction of bone marrow using magnetic beads (Park et al., 2015). To label the isolated CD34+ cells with enhanced green fluorescent protein (EGFP), CD34+ cells were cultured overnight at 37°C/5% CO_2 in a 6-well plate in HSC Proliferation Medium (Walker et al, 2012). The following day, the cells were counted and transduced at multiplicity of infection 20 with a lentiviral vector containing EGFP and luciferase. After successful transduction (>40% positive EGFP cells), the cells were frozen and stored in liquid nitrogen. In preparation for injection, the cells were thawed and cultured in HSC Proliferation Medium. They were then pelleted, washed in PBS, and then re-suspended at 50,000 cells/μL in PBS for intravitreal injection.

2.4 Intravitreal Injections

Intravitreal injections were performed 5 days after Alzet Pump implantation. All intravitreal injections were performed in the right eye pars planar under isoflurane (2–3% in oxygen) anesthesia. After instilling 5% betadine solution into the fornix, a sterile 33-G needle attached to a Hamilton syringe was used to deliver 1 μL solution per eye of either EGFP-labeled human CD34+ BMSCs (50,000 cells) or PBS (n =20 mice per groups). Following injection, Erythromycin eye ointment was applied to the injected eye.

2.5 Retinal Imaging

To assess the development of retinopathy and visualize EGFP-labeled CD34+ BMSCs, both eyes of each mouse were imaged at 1 and 4 weeks after intravitreal injection. A custom multimodal retinal imaging system designed and built for *in vivo* mouse retinal imaging was used as previously described (Zhang et al., 2015; Zhang et al, 2018). This system integrates multichannel SLO and OCT and allows simultaneous collection of complementary information, offered by these two retinal imaging modalities. The imaging system scanning head offers a retinal field of view of up to 50° and contains mouse contact lens that is in contact with the animal during imaging, allowing the mouse cornea to be kept hydrated and clear. The mouse retinal imaging was performed under isoflurane (2–3% in oxygen) inhalation anesthesia. A heating pad was used to maintain normal body temperature and avoid the development of “cold cataracts” during imaging (Bermudez et al., 2011).

2.6 SLO Subsystem

A 488 nm laser (OBIS 488LX, Coherent Inc., Santa Clara, CA, USA) is used as the light source for the SLO subsystem. The light source provides strong excitation for EGFP. a corresponding dichroic mirror (DM1; Di01-R488/561; Semrock, Inc., Rochester, NY, USA) and filter (FF01–525/45; Semrock) for EGFP emitted fluorescence light to be detected were used with a photomultiplier tube (PMT) (H7422–40; Hamamatsu Photonics, K.K., Shizuoka, Japan). A reflected light was acquired by separate PMT (H7422–20; Hamamatsu). Fluorescein angiography (FA) was performed with intravenous injection of 0.1 mL of 4mM fluorescein (AK-Fluor, Akorn Pharmaceuticals, Lake Forest, IL) after completing the SLO imaging for EGFP-labeled cells, using the same excitation and detection components.

2.7 OCT Subsystem

The imaging beam from the sample arm of the Fourier-domain (i.e., spectral domain) OCT system was optically integrated with the SLO subsystem via the second dichroic mirror (DM2, FF775-Di01, Semrock). We used a broadband light source with a 132-nm bandwidth centered at 860 nm (Broadlighter 860; Superlum Diodes Ltd., Cork, Ireland), which provides ~3.6 μm theoretical axial resolution in tissue. As Fourier-domain OCT detector, a custom spectrometer with a high-speed line CMOS camera (Sprint spL4096–140km; Basler, Ahrensburg, Germany) was used. The OCT system operates at speeds of 100,000 A-scan/s. Phase-variance OCT angiography (OCTA) was also obtained using this system (Zhang et al, 2015). Standard OCT and OCTA data processing have been applied to generate OCT and OCTA serial B-Scans.

2.8 Tissue Processing

At 1 and 4 weeks after intravitreal injections, the mice from each study group were euthanized by asphyxiation with gaseous CO_2 in a closed chamber following retinal imaging. Following euthanasia, the right eye was harvested for immunohistochemistry, wholemount preparation or microarray analysis.

2.9 Immunohistochemistry

Eyes were prepared and fixed for immunostaining as previously described (Moisseiev et al., 2016). The sections were stained with rabbit anti-GFP (Life Technologies, Carlsbad, CA, USA) and anti-human nuclei monoclonal antibody (HuNu antibody; EMD Millipore, Billerica, MA, USA) to identify human cells. After primary antibody exposure, the secondary antibody used was Alexa Fluor 647–conjugated donkey anti-mouse IgG (Millipore) and Cy3 conjugated donkey anti-rabbit IgG (Jackson ImmunoResearch Labs, West Grove, PA, USA). Confocal microscopy was performed using a laser-equipped Olympus FV 1000 Confocal microscope (Olympus America Inc, Center Valley, PA). The localization of the EGFP, DAPI and monoclonal HuNu antibody was detected and the final digital image was produced by overlapping green (EGFP), blue (DAPI) and red (HuNu antibody) fluorescent labels.

2.10 Microarray Analysis

2.10.1 RNA Isolation and labeling—Retinal tissue was collected based on a standard protocol after animal sacrifice at 1 week following intravitreal injection (Moisseiev et al., 2016). Tissue was placed in RNALater (Qiagen, Valencia, CA) and stored at −20°C. miRNeasy isolation kit (Qiagen) was used to isolate total RNA including microRNA following manufacturer's instructions. Isolated total RNAs, including microRNA, were labeled for microarray gene expression analysis following a published protocol with slight modifications (Smit-McBride et al, 2011). Isolated RNA samples were run on an Agilent BioAnalyzer microfluidics chip RNA Nano 6000 (Agilent Technologies, Santa Clara, CA, USA) to assess quality and quantity. Out of four samples, the three samples having the highest quality (RNA Integrity Number [RIN] ≥ 7 value) were labeled as probes for the Affymetrix GeneChip microarrays (Affymetrix, Santa Clara, CA, USA). Samples of RNA were labeled using 50 ng total RNA, following the manufacturer's protocol for GeneChip WT Terminal Labeling and Controls Kit (Affymetrix) combined with Ambion WT Expression Kit (Ambion, Inc., Foster City, CA, USA). After labeling, the probes were hybridized to the Affymetrix Mouse Transcriptome Array 1.0 (MTA1) GeneChip microarrays. This array analyzes the expression of >114,000 transcripts for protein coding genes and >101,000 transcripts for nonprotein coding content (noncoding RNA, such as microRNA, pseudogenes, and rRNA). Hybridization was performed at the Genomics Shared Resource at UC Davis Medical Center using a standard manufacturer's procedure (Affymetrix). The total dataset included 6 GeneChip microarrays.

2.10.2 Microarray Data Analysis—Microarray data were analyzed using Affymetrix Expression Console followed by Transcriptome Analysis Console 3.0.. Microarray raw, processed, and metadata was submitted to NCBI GEO database, with Accession Number

GSE138719. Pathways analysis was done using Ingenuity Pathway Analysis software (IPA, Qiagen), for identification of biologically relevant changes of expression in genes and related pathways of the retina. One-way ANOVA was used in the Transcriptome Analysis Console to identify statistically significant genes at a significance level of $P \leq 0.05$. We used the standard approach of using a dual criterium of P-value ≤ 0.05 and fold change (FC) $-1.5 \geq FC \geq 1.5$ to identify differentially expressed genes. This approach ensures control of false positive candidates and preserves the desired biological significance.

2..11 Wholemount preparation and immunostaining

After fixing whole eyes in 4% paraformaldehyde in PBS at 4 °C for 1 hour, the retina was dissected and flat-mounted, and fixed under coverslips overnight in cold paraformaldehyde (Soto et al., 2008). After graded series of washes in PBS, 33, 66 and 100% methanol, the retina was stored at −20° C in 100% methanol. The reverse graded series of methanol was used to rehydrate the retinas prior to antibody labeling. After blocking in 5% normal donkey serum in PBS with 0.3% TritonX-100, retinas were incubated for 24hrs at 4° C with 1:250 Alexa Fluor-647 conjugated Isolectin-GS-IB4 from Griffonia simplicifolia (Invitrogen I32450, lot 1874784). After additional washes in PBS, the retina was mounted on a slide using Aqua Poly/Mount (Polysciences).

The flat-mounted retina was imaged in their entirety using a 20× Plan-Apochromat 0.8NA objective using a 200M Zeiss microscope controlled by IPlab software. At each position, multiple images were acquired at different z-positions for the whole retina thickness for the IB4 signal. After making maximum intensity projections for each channel, retina mosaics were created.

2.12 Retinal vascular density analysis

Vascular density of the retinal flat mount was quantitated using ImageJ software (https://imagej.nih.gov, National Institute of Health, Bethesda, Maryland) with Vessel Analysis plugin as described previously (Zarb et al, 2019). This plugin automatically measures the density, length and diameter of retinal vasculature. Vascular density is defined as the ratio of vasculature area to the total selected area and is reported as % Area. Student paired t-test was used for statistical analysis and a P value less than 0.05 was considered significant.

3. RESULTS

The time course for the development of retinopathy was studied in STZ-induced diabetic mice a total of 3 times. Based on *in vivo* retinal imaging analysis, reproducible early retinal vascular changes consistent with diabetic retinopathy could be detected in these mice starting at 5 months after induction of diabetes that progressed close to a plateau by month 6 and remained stable up to 8 months. The in vivo retinal imaging retinal microvascular changes included patches of retinal non-perfusion visualized using OCTA and early phase FA, i.e. within 5 minutes after intravenous fluorescein injection (Fig 1A, 2A), and diffuse late leakage noted on late phase FA, i.e. 20 minutes after intravenous injection of fluorescein dye (Robinson et al, 2012). These retinal vascular changes on OCTA and FA were not observed in age-matched wild-type non-diabetic C57BL/6J mice. Based on this finding, 5 to

5.5 months after induction of diabetes was determined the ideal time-point for cell therapy intervention since the goal of cell therapy was to intervene at the earliest sign of development of diabetic retinopathy in order to maximize the potential protective effects.

3.1 In Vivo Retinal Imaging

At 1 week after intravitreal injection, FA and OCTA of each eye demonstrated retinal microvascular changes including areas of retinal capillary non-perfusion consistent with early diabetic retinopathy (Fig. 1A, 2A). No neovascularization was seen. The extent of these retinal microvascular changes was relatively symmetric in both eyes and similar among mice in study groups.

Fundus fluorescence SLO imaging, carried out prior to fluorescein injection, detected fluorescence consistent with EGFP-labeled cells in the eye 1 week after intravitreal injection of EGFP-labeled CD34+ BMSCs. Fluorescence was observed on SLO fundus imaging in the region of the retina with retinal microvascular abnormalities seen on FA (Fig. 1B). The plausible axial locations of EGFP-labeled cells were determined using combined OCT and SLO imaging. Multiple hyper-reflective spots were detected at the vitreo-retinal interface in the eyes injected with CD34+ BMSCs that co-localized with the EGFP signal seen on SLO (Fig. 1C). Some of these hyper-reflective signals clustered along flow signals from retinal blood vessels detected on OCTA, but others were found in the regions of the retina without detectable retinal blood flow on OCTA (Fig. 1D). In contrast, eyes that received PBS injection showed minimal background fluorescence on SLO fundus imaging (Fig. 2B); the retinal surface was smooth and devoid of any cell-like hyper reflective material on OCT (Fig. 2C & D). Similar observations were noted 4 weeks after intravitreal injection. In age-matched non-diabetic wildtype mice with systemic immunosuppression, intravitreal injection of EGFP-labeled CD34+ BMSCs did not show any EGFP-labeled cells on SLO or OCT imaging of the retina after 1 and 4 weeks.

3.2 Immunohistochemical Analysis

Eyes were harvested and sectioned for immunohistochemistry 1 and 4 weeks after intravitreal injection to detect the human cells. While only background staining was present in PBS injected control group (Fig. 3A), cells with annular HuNu staining consistent with human cells were detected on the surface of the retina (Fig. 3B & C arrows) and along the some of the retinal vasculature (Fig. 3C arrowheads). These cells were labeled with EGFP. In some eyes, EGFP labeled cells were also detected at the inner layers of the retina and around retinal vessels without HuNu staining. (Fig. 3B, arrowheads). These cells likely represent human cells that did not stain with HuNu due to the limited tissue penetration of the antibody.

3.3 Microarray Analysis of the Retina

Retinas from injected murine eyes were harvested for microarray analysis at 1 week following intravitreal injection. The RNA samples were analyzed for statistically significant changes in gene expression (i.e., $-1.5 \geq FC \geq 1.5$ and $P < 0.05$). Expression of 162 murine genes were significantly changed following cell injection when compared to PBS injection. Analysis through Ingenuity Pathways Analysis (IPA) software identified that the top

canonical pathways that were significantly affected were the inflammatory pathways including Toll-like receptor, MAP kinase, oxidative stress, cellular development, assembly and organization pathways (Fig. 4). Supplemental table provides a summary of data of the fold changes of the genes used for heatmap and IPA analysis

3.4 Retinal vascular analysis

In order to investigate the effects of CD34+ BMSCs on the retinal vasculature in these eyes with diabetic retinopathy, retinal vascular density analysis was conducted using flat-mounts of murine retina 4 weeks after intravitreal injection (Fig. 5). The mean retinal vascular density was 11.41±1.60 for the PBS-injected group (n=12) and 13.39± 2.53 for the CD34+ cell-injected group (n=9). The retinal vascular density was significantly higher in CD34+ cell-injected eyes when compared to PBS injected eyes ($P<0.03$).

4. DISCUSSION

This study used a murine model of diabetic retinopathy to characterize the effects of intravitreal injection of human CD34+ BMSCs on the retina and determine whether the effects may be protective. Human CD34+ BMSCs were studied since they contain both endothelial progenitor cells that directly engraft into the retinal vasculature and HSCs that can have protective effects on the retina with diabetic retinopathy via paracrine mechanisms (Park et al., 2017; Rong et al., 2018). The rationale for this study is based on previous preclinical work showing that intravitreal injection of circulating human CD34+ cells is associated with rapid retinal vascular homing of these cells in eyes with diabetic retinopathy or retinal ischemia-reperfusion injury suggestive of repair (Caballero et al., 2007). Although long-term effects of the CD34+ cell injection was not studied, potential reparative effects of the CD34+ cells on the damaged retinal vasculature was speculated. Using NOD-SCID mice with acute retinal ischemia-reperfusion injury, our group later showed long-term retinal vascular integration of human cells following intravitreal injection of human CD34+BMSCs without abnormal proliferation of human cells in the eye or systemically (Park et al., 2012). The retinal vasculature appeared normalized long-term, but the potential protective or regenerative effects of CD34+ cells could not be clearly demonstrated in this model of transient retinal vascular damage.

In this study, we used a murine model of diabetic retinopathy which is characterized by chronic progressive retinal vascular damage. STZ-induced murine model of diabetic retinopathy was used since this is a commonly used model of diabetic retinopathy with the phenotype well-characterized (Robinson et al., 2012). A reproducible and predictable time course of development of diabetic retinopathy was noted in our study using this model and in vivo retinal imaging. The time course for development of diabetic retinopathy is similar to that observed by others using fluorescein angiography (Caballero et al., 2007; Caballero et al, 2013). Prior studies using trypsin digested analysis of the retinal vasculature have shown progressive increase in acellular capillaries between 6 and 18 months after induction of diabetes mellitus in this model (Feit-Leetchman et al., 2005). However, the development of acellular capillaries are late histologic changes in this chronic condition. Since our study aimed to intervene with cell therapy at the earliest stage of development of diabetic

retinopathy, we used in vivo retinal imaging perfusion changes to detect the early changes in the retinal microvasculature.

To assess the effects of intravitreal CD34+ BMSCs on the retina with diabetic retinopathy, various methods were used. In vivo retinal imaging was used to evaluate the homing and migration of the CD34+ cells to the retina following intravitreal injection. Microarray analysis was used to study the molecular changes in the murine retina in response to CD34+ cell injection. Immunohistochemical analysis of the retina and retinal flat mount was used to identify human cells in the retina, visualize the retinal vasculature and quantitate changes in retinal vascular density.

Both in vivo retinal imaging and immunohistochemistry confirmed homing and integration of the CD34+ BMSCs to the retinal surface as well as the retinal vasculature after intravitreal injection. The rapid homing of these human cells into the damaged portion of the retinal vasculature has been previously described using circulating CD34+ cells and consistent with our study findings (Caballero et al., 2007; Caballero et al, 2013). The homing of these CD34+ BMSCs to the non-vascular portion of the retina and retinal surface is a new observation which appeared more pronounced than the retinal vascular homing noted previously.

In addition to retinal homing, the intravitreal injection of CD34+ BMSCs was associated with gene expression changes in the murine retina based on microarray analysis. Major pathways that control inflammatory response, cellular growth, proliferation, maintenance as well as cell-cell signaling and interaction were affected in the murine retina. The inflammatory pathways affected include MAP kinase, Toll-like receptor, and oxidative stress response. Many of these pathways have been implicated to play a role in the pathogenesis of diabetic retinopathy (Semeraro et al., 2015). These microarray changes are different from those observed following intravitreal CD34+ BMSCs injection in rd1 mice with retinal degeneration although the same human cells were injected into murine eyes (Moisseiev et al., 2016), Although microarray analysis data are descriptive, it is of note that the molecular changes induced in the murine retina following intravitreal injection of CD34+ BMSC appear to vary depending on the pathologic process in the retina that the CD34+ cells are responding to.

To assess the effects of CD34+ BMSCs on the retinal vasculature in eyes with diabetic vasculopathy, we measured the retinal vascular density using immunohistochemistry of flat-mount of the murine retina and ImageJ software. This was done 4 weeks after intravitreal CD34+ BMSC injection. Our analysis demonstrated preservation of the retinal vessels following intravitreal injection of CD34+ BMSCs (Figures 5). Longer follow-up study could not be performed since the mice did not tolerate longer systemic immunosuppression (personal observation).

The current preclinical study was conducted to characterize further the effects of intravitreal CD34+ BMSCs in eyes with diabetic retinopathy before exploring efficacy of this cell therapy in a large clinical trial for diabetic retinopathy. We have conducted a small early phase clinical trial showing safety and feasibility of intravitreal injection of autologous

CD34+ BMSCs in eyes with various ischemic and degenerative retinal disorders (Park et al., 2015). Others showed safety of intravitreal injection of the mononuclear cell fraction of bone marrow, a crude cell mixture that contains mostly blood cells and very few CD34+ cells (Park et al, 2017; Siqueira et al, 2015).

Although our current study used CD34+ BMSCs from a healthy donor and demonstrated potential positive therapeutic effects. it is important to note that previous preclinical studies showed that circulating CD34+ cells from diabetic individuals have defective retinal homing (Caballero et al., 2007; Caballero et al, 2013). Future studies using CD34+ BMSCs from a diabetic donor may provide more insight regarding whether autologous CD34+ BMSCs can be used for diabetic retinopathy.

In our current study, human CD34+ BMSCs were isolated from the mononuclear cellular fraction of the bone marrow aspirate using a magnetic cell sorter, similar to the established protocol used for the clinical trial (Park et al., 2015). The harvested CD34+ cells were labeled with EGFP prior to intravitreal injection in order to trace the migration of these cells in the eye using in vivo retinal imaging and immunohistochemistry. The study demonstrates that human CD34+ BMSCs can migrate and integrate into the retinal surface, along retinal vasculature and in the regions of avascular retina. Since CD34+ cells include endothelial progenitor cells, some cells are expected to home into the retinal vasculature as reported previously (Caballero et al., 2007; Park et al, 2012; Caballero et al, 2013). The presence of these cells in flow-void zones of the retina on OCT/OCTA imaging is noteworthy and support potential neuroprotective effects of these cells via paracrine effects (Li et al., 2006; Park et al., 2017).

There are important aspects of this current study that make it unique when compared with previous works. Previous cross-species preclinical studies used circulating CD34+ cells from peripheral blood and evaluated short term (48 hours) response using cyclosporine for immunosuppression (Caballero et al, 2007). In our study, we used a more complete systemic immunosuppressive regimen for the 4-week study duration to minimize rejection and optimize viability and sustainability of the human cells in the eye (Moisseiev et al., 2016). Since CD34+ cells in bone marrow are found in high concentration and potentially less affected by systemic factors, we used BMSCs rather than circulating cells. While previous studies concentrated on the homing of CD34+ cells to the retinal vasculature (Caballero et al, 2007), we took advantage of our advanced custom retinal imaging apparatus to study the homing and migration of these cells in the retina in live eyes. On immunohistochemistry and in vivo imaging, the retinal homing of the CD34+ BMSCs do not appear to be limited to the retinal vasculature. Finally, we examined the delayed effect of CD34+ BMSC on retinal vasculature and noted the preservation of retinal vasculature in eyes with diabetic retinopathy.

This study has some limitations. First, continuous systemic immunosuppression was used which could influence the development of diabetic retinopathy or the behavior of CD34+ BMSCs. In our study, diabetic retinopathy progressed as expected during the 4-week follow-up in PBS treated control eyes and the contralateral untreated left eye despite chronic systemic immunosuppression. Multiple inflammatory pathways that play a role in the

pathogenesis of diabetic retinopathy were affected by CD34+ BMSC injection on microarray analysis despite immunosuppression. These microarray changes unlikely represent an inflammatory rejection of human cells since inflammatory pathways were not affected on microarray analysis of the retina of rd1 mice following intravitreal injection of the same CD34+ BMSCs (Moisseiev et al., 2016). Furthermore, the affected pathways in the diabetic retina were limited to those implicated in the pathogenesis of diabetic retinopathy and are different from pathways that were affected in rd1 mice with retinal degeneration following intravitreal human CD34+ BMSC injection. Secondly, STZ-induced model of diabetic retinopathy is a commonly used preclinical model, but it does not fully replicate human disease. For example, retinal neovascularization is not observed in this model and the development of neuronal loss is not consistently observed (Feit-Letchman et al., 2005; Robinson et al., 2012). Thus, some caution is prudent when extrapolating our study observations to human eyes with diabetic retinopathy. In the model of STZ-induced diabetic retinopathy used in our current study, retinal neuronal loss appeared minimum using in vivo imaging and immunohistochemistry (personal observations). This is consistent with prior observations using this model (Feit-Letchman et al., 2005). Thus, we limited our quantitative analysis to the retinal vasculature,

The goal of our study was to intervene with intravitreal CD34+ BMSCs at the earliest detectable stage of diabetic retinopathy in this murine model since early intervention may have a more demonstrable protective effects on the retinal vasculature. Whether the protective effects of CD34+ cells on retinal vasculature in eyes with diabetic retinopathy results from regeneration of the damaged retinal vasculature or from minimizing any further damage associated diabetes mellitus is unknown at the current time. Future studies will be needed to determine fully the mechanism of action of these CD34+ cells. Longer follow-up study could not be performed using our murine model since the mice did not tolerate longer period of systemic immunosuppression (personal observations).

5. CONCLUSIONS

In a murine mode of diabetic retinopathy and systemic immunosuppression, intravitreal injection of human CD34+ BMSCs results in homing and integration of these human cells in the retina. This is associated with preservation of the retinal vasculature and molecular changes in the retina for pathways implicated to play a role in the pathogenesis of diabetic retinopathy.

Supplementary Material

Refer to Web version on PubMed Central for supplementary material.

Acknowledgment:

The authors thank Sharon L. Oltjen for immunohistochemistry, Missy T. Pham for assistance with stem cells preparation, Dr. Suman K. Manna, and Dr. Ratheesh K. Meleppat for collecting and processing some of the *in vivo* retinal imaging data, and Drs. Jonathan Lu and Parisa Emami for their help with intravitreal injection during the early phase of this study. The research findings have been presented in part as paper presentations at the annual meetings of ARVO (2018, Honolulu and 2019, Vancouver) and Retina Society (2018, San Francisco).

Funding: This research was supported by EY026556 (RJZ), and NEI core (P-30 EY012576) and Barr Foundation for Retinal Research (ZSM, RJZ)

Abbreviations:

BMSCs	bone marrow stem cells
EGFP	enhanced green fluorescent protein
FA	fluorescein angiography
FC	fold change
HSC	hematopoietic stem cell
HuNu	human nuclei
OCT	optical coherence tomography
OCTA	optical coherence tomography angiography
PBS	phosphate buffered saline
SD-OCT	spectral domain optical coherence tomography
SLO	scanning laser ophthalmoscopy
STZ	streptozotocin

References

Bermudez MA, Vicente AF, Romero MC, Arcos MD, Abalo JM,Gonzalez F, et al., 2011 Time course of cold cataract development in anesthetized mice. Curr. Eye Res 36, 278–284. 10.3109/02713683.2010.542868 [PubMed: 21275518]

Caballero S, Sengupta N, Afzal A, Chang KH, Calzi SI, Guberski DL, et al., 2007 Ischemic vascular damage can be repaired by healthy, but not diabetic, endothelial progenitor cells. Diabetes 56, 960–967. https://doi: 10.2337/db06-1254 [PubMed: 17395742]

Caballero S, Hazra S, Bhatwadekar A, Calzi SI, Paradiso LJ, Miller LP, et al., 2013 Circulating mononuclear progenitor cells: differential roles for subpopulations in repair of retinal vascular injury. Invest. Ophthalmol. Vis. Sci 54, 3000–3009. https://doi:10.1167/iovs.12-10280 [PubMed: 23572102]

Eezquer M, Urzua CA, Montecino S,Leak K, Conget P, Ezquer F, 2016 Intravitreal administration of multipotent mesenchymal stromal cells triggers a cytoprotective microenvironment in the retina of diabetic mice. Stem Cell Res. Ther 7: 42. https:// doi: 10.1186/s13287-016-0299-y. [PubMed: 26983784]

Feit-Letchman RA, Kinouchi R, Takeda M, Fan Z, Mohr S, Kern TS, et al., 2005 Vascular damage in a mouse model of diabetic retinopathy: relation to neuron and glial changes. Invest. Ophthalmol. Vis. Sci 46, 4281–4287. https:// doi:10.1167/iovs.04-1361 [PubMed: 16249509]

Frljak S, Jaklic M, Zemljic G, Cerar A, Poglagen G, Vrtovec B, 2018 CD34+ Cell transplantation improves right ventricular function in patients with nonischemic dilated cardiomyopathy. Stem Cells Transl. Med 7, 168–172. https:// doi: 10.1002/sctm.17-0197 [PubMed: 29380563]

Gu X, Yu X, Zhao C, Duan P, Zhao T,Liu Y, et al., 2018 Efficacy and safety of autologous bone marrow mesenchymal stem cell transplantation in patients with diabetic retinopathy. Cell Physiol. Biochem 49: 40–52. https:// doi: 10.1159/000492838. [PubMed: 30134223]

Kocur I, Resnikoff S, 2002 Visual impairment and blindness in Europe and their prevention. Br. J. Ophthalmol 86, 716–722. [PubMed: 12084735]

Li Y, Reca RG, Altmaca-Somnez P, Ratajczak MZ, Ildstad ST,Kaplan HJ, et al., 2006 Retinal pigment epithelium damage enhances expression of chemoattractants and migration of bone marrow–derived stem cells. Invest. Opthalmology Vis. Sci 47, 1646–1652. https://doi:10.1167/iovs.05-1092

Mackie AR, Losordo DW, 2011 CD34-positive stem cells: in the treatment of heart and vascular disease in human beings. Texas Hear. Inst. J 38, 474–485.

Moisseiev E, Smit-McBride J, Oltjen S, Zhang P, Zawadzk RJ, Motta M, et al., 2016 Intravitreal administration of human bone marrow CD34+ stem cells in a murine model of retinal degeneration. Invest. Opthalmology Vis. Sci 57, 4125–4135. https://doi:10.1167/iovs.16-19252

Oner A, Gonen ZB, Sinim N, Cetin M, Ozkul Y, 2016 Subretinal adipose tissue-derived mesenchymal stem cell implantation in advanced stage retinitis pigmentosa: a phase 1 clinical safety study. Stem Cell Res. Ther 7, 178 [PubMed: 27906070]

Park SS, Caballero S, Bauer G, Shibata B, Roth A, Fitzgerald PG et al., 2012 Long-term effects of intravitreal injection of GMP-grade bone-marrow-derived CD34+ cells in NOD-SCID mice with acute ischemia-reperfusion injury. Invest. Ophthalmol. Vis. Sci 53, 986–994.https:// doi: 10.1167/iovs.11-8833 [PubMed: 22247454]

Park SS, Bauer G, Abedi M, Pontow S, Panorgias A, Jonnel R, et al., 2015 Intravitreal autologous bone marrow CD34+ cell therapy for ischemic and degenerative retinal disorders: preliminary phase 1 clinical trial findings. Invest. Ophthalmol. Vis. Sci 56, 81–89. https:// doi: 10.1167/iovs.14-15415

Park SS, Moisseiev E, Bauer G, Anderson JD, Grant MB, Zham A, et al., 2017 Advances in bone marrow stem cell therapy for retinal dysfunction. Prog. Retin. Eye Res 56, 148–165. https:// doi: 10.1016/j.preteyeres.2016.10.002 [PubMed: 27784628]

Robinson R, Barathi VA, Chaurasia SS, Wong TY, Kern TS, 2012 Update on animal models of diabetic retinopathy: from molecular approaches to mice and higher mammals. Dis. Model. Mech 5, 444–456. https:// doi: 10.1242/dmm.009597 [PubMed: 22730475]

Rong L, Gu X, Xie J, Zeng Y, Li Q, Chen S, et al., 2018 Bone marrow CD133+ stem cells ameliorate visual dysfunction in streptozotocin-induced diabetic mice with early diabetic retinopathy. Cell Transplant. 27, 916–936. https:// doi: 10.1177/0963689718759463 [PubMed: 29717657]

Semeraro F Cancarini A, dell'Omo R, Rezzola S, Romano MR, Costagliola C, 2015 Diabetic Retinopathy: vascular and Inflammatory disease. J. Diabetes Res 582060. https:// doi: 10.1155/2015/582060

Siqueira RC, Messias A, Voltarelli JC, Scott IU, Jorge R, 2011 Intravitreal injection of autologous bone marrow-derived mononuclear cells for hereditary retinal dystrophy. Retina. 31, 1207–1214. https:// doi: 10.1097/IAE.0b013e3181f9c242 [PubMed: 21293313]

Smit-McBride Z, Modjtahedi SP, Cessna CT, Telander DG, Hjelmeland LM, Morse LS., 2011 In vivo gene expression profiling of retina postintravitreal injections of dexamethasone and triamcinolone at clinically relevant time points for patient care., Invest Ophthalmol Vis Sci., 11 21;52(12):8965–78. [PubMed: 21873667]

Smit-McBride Z, Modjtahedi SP, Cessna CT, Telander DG, Hjelmeland LM, Morse LS., 2011 In vivo gene expression profiling of retina postintravitreal injections of dexamethasone and triamcinolone at clinically relevant time points for patient care., Invest Ophthalmol Vis Sci., 11 21;52(12):8965–78. [PubMed: 21873667]

Soto I, Oglesby E, Buckingham BP, Son JL, Roberson EDO, Steele MR, et al., 2008 Retinal ganglion cells downregulate gene expression and lose their axons within the optic nerve head in a mouse glaucoma model. J. Neurosci 28, 548–561. 10.1523/JNEUROSCI.3714-07 [PubMed: 18184797]

Walker JE, Chen RX, McGee J, Nacey C, Pollard RB, Abedi M, et al., 2012 Generation of an HIV-1-resistant immune system with CD34(+) hematopoietic stem cells transduced with a triple-combination anti-HIV lentiviral vector. J. Virol 86, 5719–5729. https://doi: 10.1128/JVI.06300-11 [PubMed: 22398281]

Wang JD, An Y, Zhang JS, Wan XH, Jonas JB, Xu L, et al., 2017 Human bone marrow mesenchymal stem cells for retinal vascular injury. Acta Ophthalmol. 95, e453–461. https:// doi: 10.1111/aos.13154 [PubMed: 27807930]

Zarb Y, Weber-Stedlbauer U, Kirshenbaum D, Kindler DR, Richetto J, Keller D, et al., 2019 Ossified blood vessels in primary familial brain calcification elicit a neurotoxic astrocyte response. Brain 142, 885–902. 10.1093/brain/awz032 [PubMed: 30805583]

Zhang P, Zam A, Jian Y, Wang X, Li Y,Lam KS, et al., 2015 In vivo wide-field multispectral scanning laser ophthalmoscopy–optical coherence tomography mouse retinal imager: longitudinal imaging of ganglion cells, microglia, and Müller glia, and mapping of the mouse retinal and choroidal vasculature. J. Biomed. Opt 20, 126005 10.1117/1.JBO.20.12.126005 [PubMed: 26677070]

Zhang P, Mocci J, Wahl DJ, Meleppat RK, Manna SK, Quintavalla M, et al., 2018 Effect of a contact lens on mouse retinal in vivo imaging: Effective focal length changes and monochromatic aberrations. Exp. Eye Res 172, 86–93. 10.1016/j.exer.2018.03.027 [PubMed: 29604280]

Zheng Y, He M, Congdon N, 2012 The worldwide epidemic of diabetic retinopathy. Indian J. Ophthalmol 60, 428–431. https://doi: 10.4103/0301-4738.100542 [PubMed: 22944754]

Highlights:

- Intravitreal human CD34+ cells home into murine retina with diabetic retinopathy.
- CD34+ cells alter molecular pathways associated with diabetic retinopathy pathogenesis.
- Human CD34+ cells preserve retinal vasculature in diabetic retinopathy.

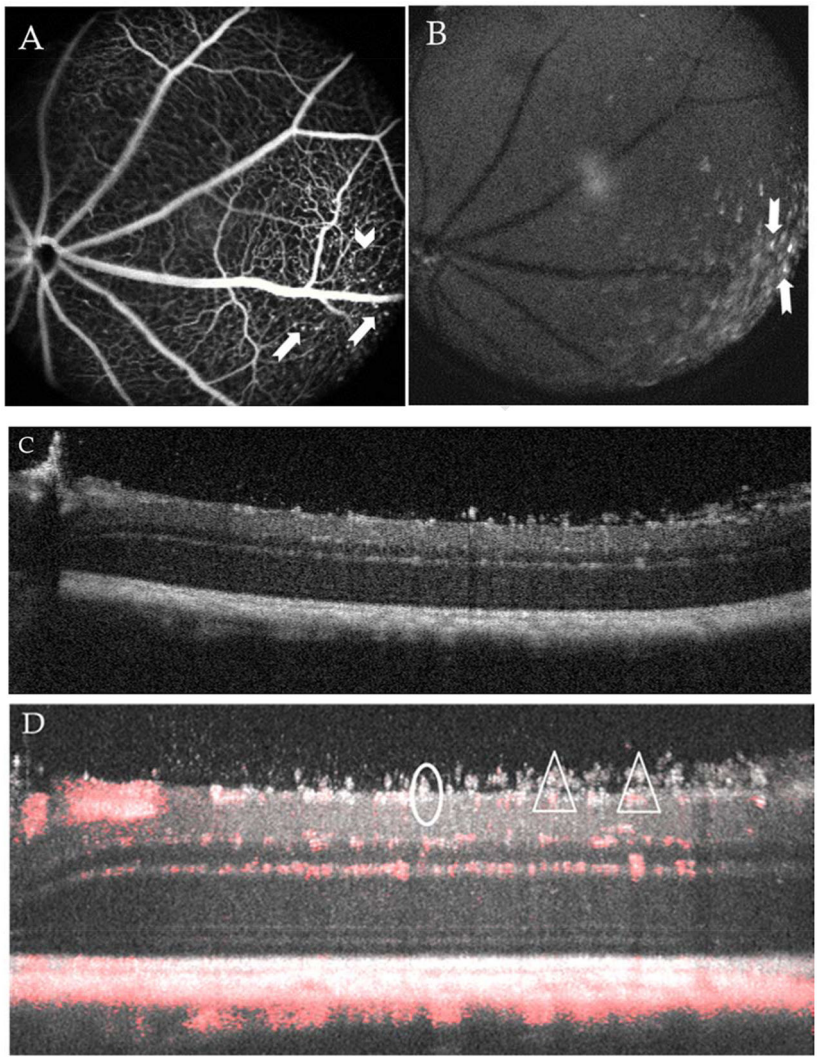

Figure 1.

In vivo multimodal retinal imaging of murine eye with STZ-induced diabetic retinopathy 1 week after intravitreal injection of EGFP-labeled CD34+ cells from a healthy human bone marrow donor. **(A)** Fluorescein angiography (FA) showing early signs of diabetic retinopathy consisting of microvascular changes including capillary non-perfusion (arrowhead; arrows). **(B)** SLO fundus imaging detected GFP signals that likely represents CD34+ cells in the region of the retina with diabetic retinopathy detected on FA. **(C)** Cross-sectional B-scan optical coherence tomography (OCT) of the retina shows hyper-reflective clumps of spots, likely cells, on the surface of the retina that colocalize to the fluorescent signal detected on the SLO fundus image. **(D)** Merged OCT/OCT angiography (OCTA) cross-sectional image of the retina showing the hyper-reflective spots (likely CD34+ cells) relative to retinal blood flow. The red color shows retinal vascular flow. Some of the hyper-reflective spots cluster around the retinal blood vessels (Triangle) while some congregate in the regions of the retina without visible vascular flow on OCTA (circle).

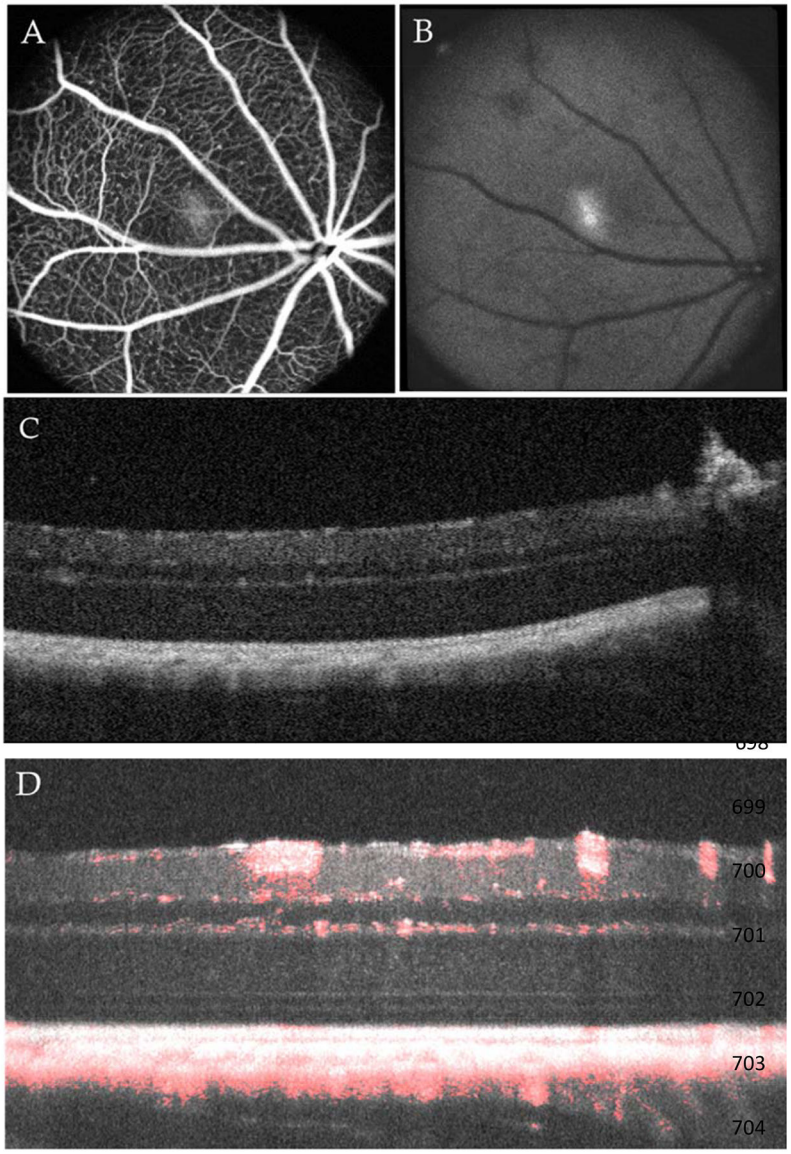

Figure 2.

In vivo multimodal retinal imaging of murine eye with STZ-induced diabetic retinopathy 1 week after intravitreal injection of PBS. **(A)** Fluorescein angiogram showed early signs of diabetic retinopathy consisting of microvascular change including capillary non-perfusion, similar to findings in Figure 1A. **(B)** The SLO fundus image does not show any GFP signal in this PBS injected eye. **(C)** Cross-sectional B scan OCT of the retina at 1 week shows a smooth retinal surface without hyper-reflective spots. **(D)** Merged OCT/OCTA cross-sectional image of the retina showing lack of hyper-reflective spots on the retinal surface suggestive of cellular material. The red color on OCTA shows retinal vascular flow.

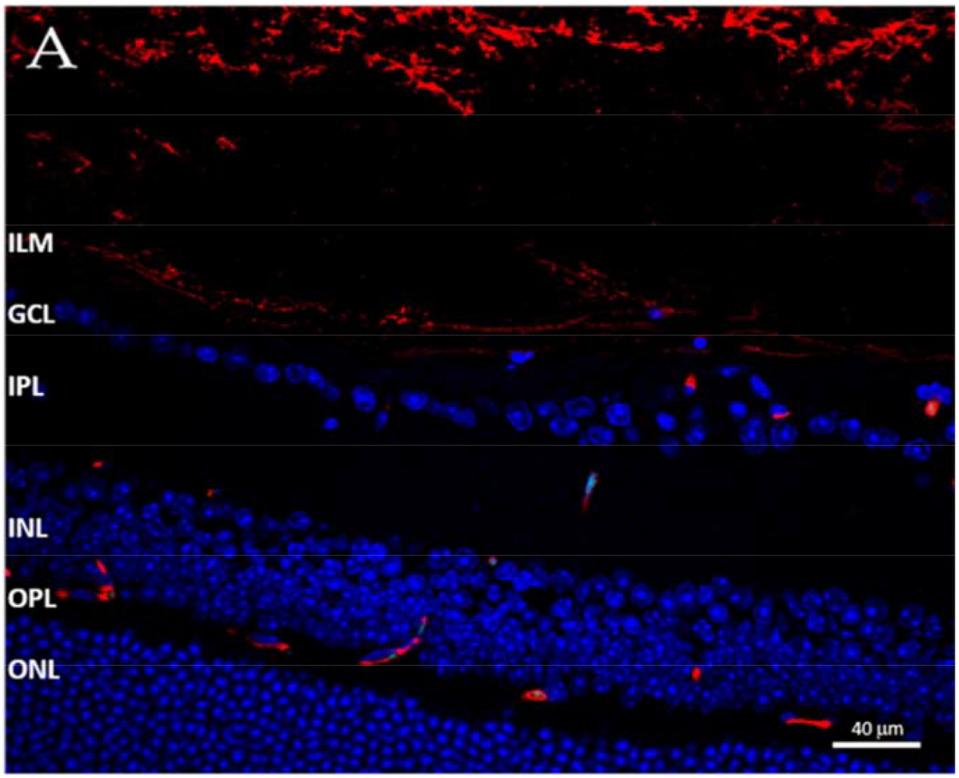

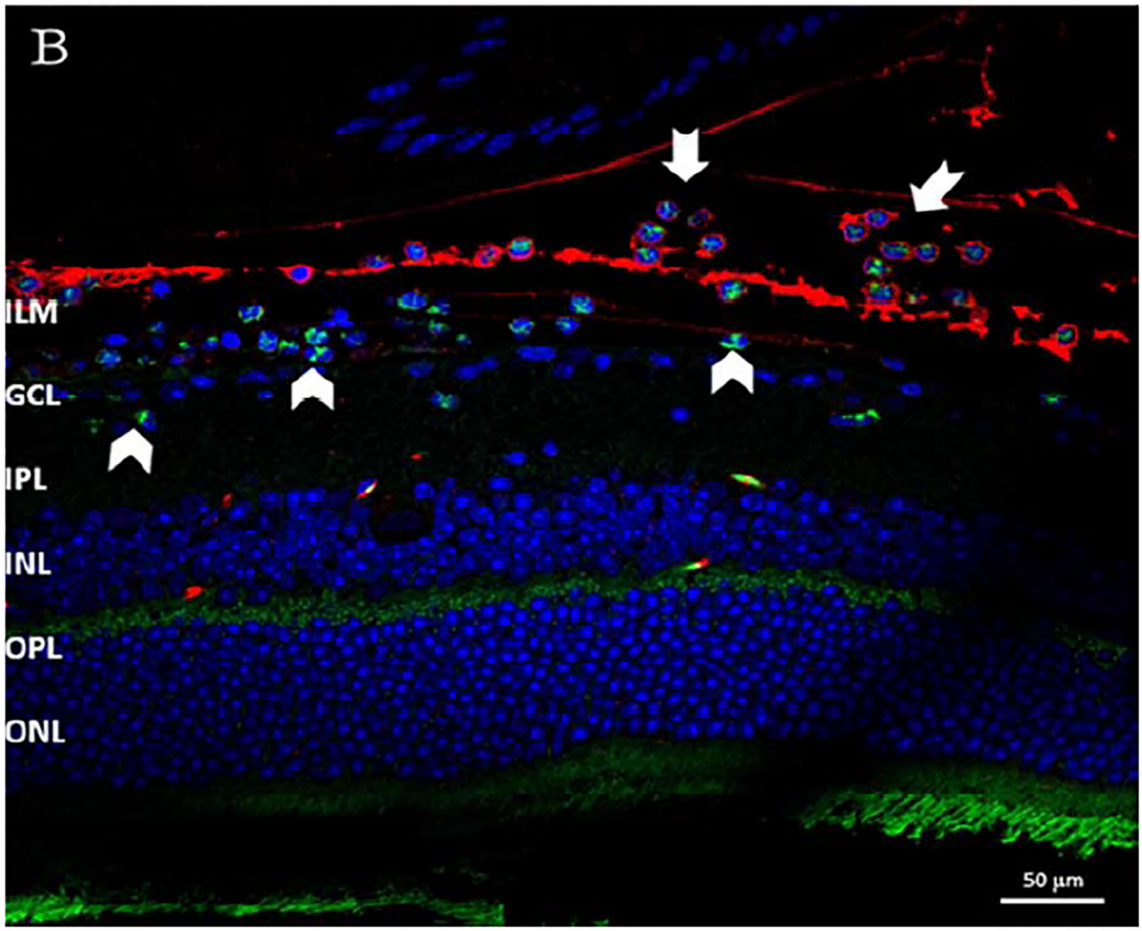

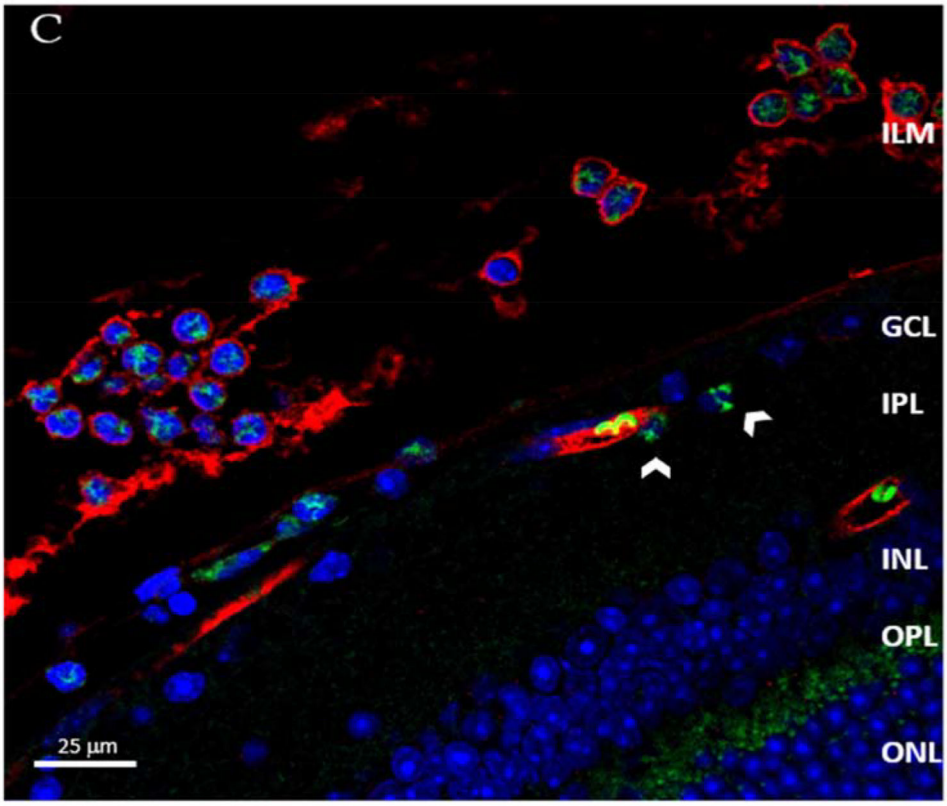

Figure 3.

Immunohistochemical analysis of the retina of the murine eye with STZ-induced diabetic retinopathy following intravitreal injection of PBS **(A)** or EGFP-labeled CD34+ cells **(B & C)**. Monoclonal HuNu antibody was used to stain human cells. Confocal microscopy performed. Blue channel (DAPI), green (EGFP) and red (HuNu antibody). Human cells detected on the retinal surface by annular red staining of cells (Arrows; (**B & C**). Additionally, some cells that only stained for EGFP (green; arrow heads; **B**) are noted in the inner retinal layers and around retinal vasculature (star; **C**) which likely represent human CD34+ cells. Two red blood cells with green autofluorescence are visible inside the lumen of the vessel in this picture (star; **C**).

A

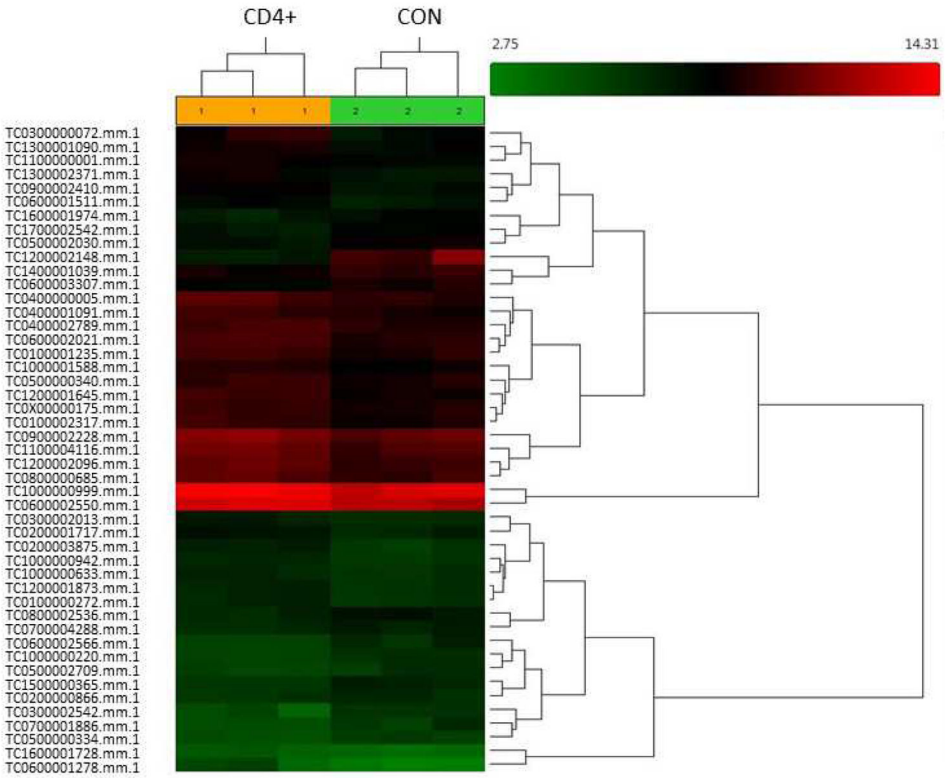

B

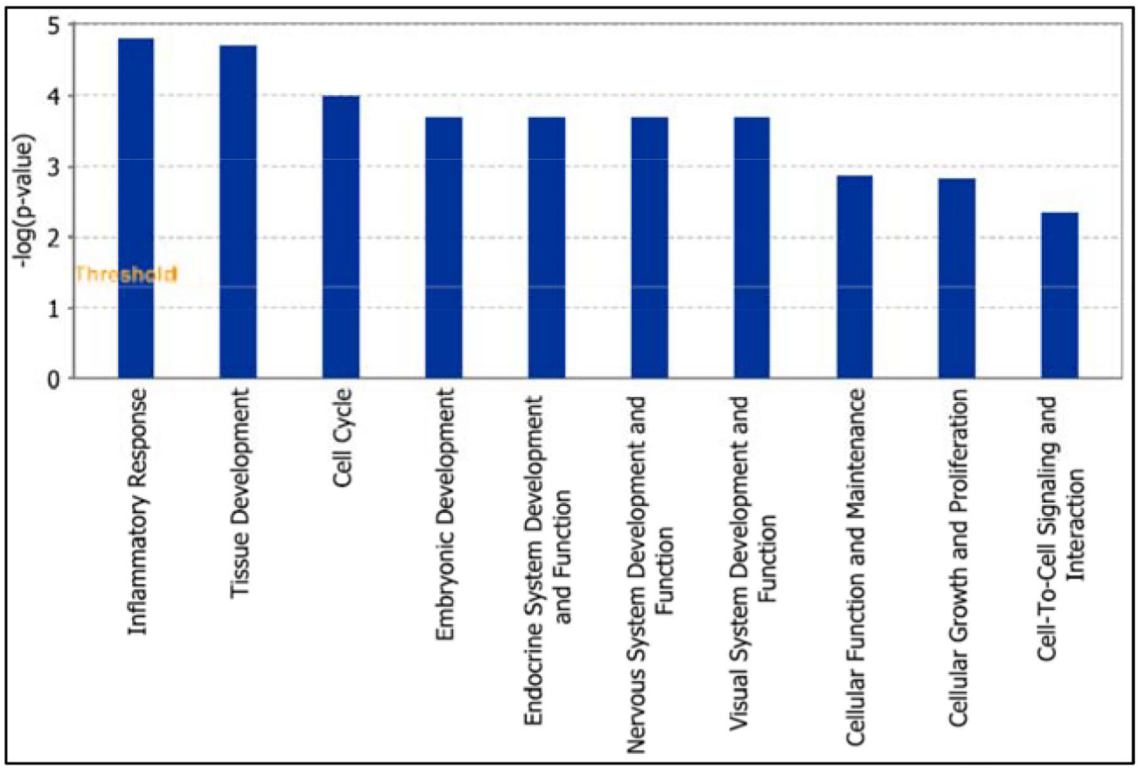

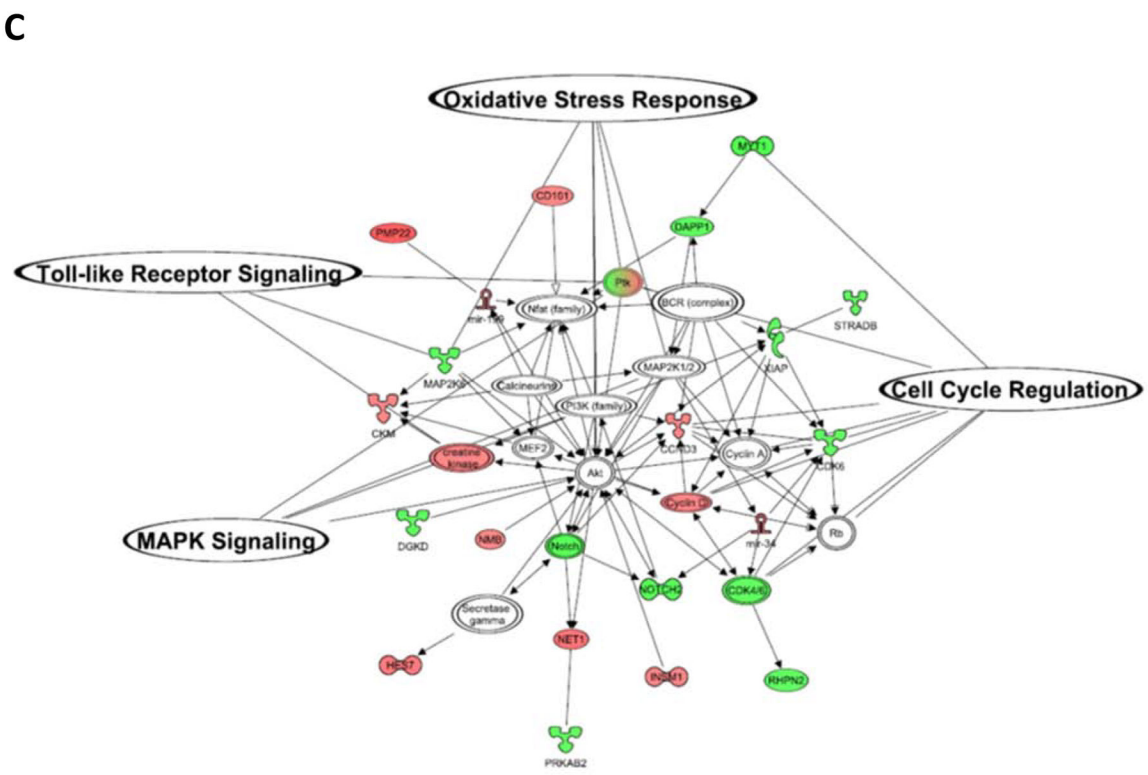

Figure 4.

Microarray analysis of gene expression changes in the murine retina after CD34+ cell injection. Transcriptome Analysis Console (TAC) 3.0 software was used to identify and cluster differentially expressed genes (heatmap, A, TC1200002148.mm.1 (Dio2, deiodinase, iodothyronine, type II); TC0300002542.mm.1 (Gm17651, predicted gene, 17651); TC0500002709.mm.1 (Gm11115, predicted gene 11115); TC0700001886.mm.1 (Bag3, BCL2-associated athanogene 3); TC1600001974.mm.1 (Adamts1, a disintegrin-like and metallopeptidase (reprolysin type) with thrombospondin type 1 motif, 1, Complex); TC0600002566.mm.1 (NonCoding); TC1700002542.mm.1 (Gm26124, predicted gene, 26124); TC1000000220.mm.1 (Gm22566, predicted gene, 22566); TC0800002536.mm.1 (Gm4899, predicted gene 4899, Complex); TC0700004288.mm.1 (Nupr1, nuclear protein transcription regulator 1; nuclear protein 1, Complex); TC1500000365.mm.1 (Gm23530, predicted gene, 23530); TC0200000866.mm.1 (Gm13527, predicted gene 13527, glyceraldehyde-3-phosphate dehydrogenase (Gapdh) pseudogene); TC1400001039.mm.1 (Gm21750, predicted gene, 21750); TC0500000334.mm.1 (Fosl2, fos-like antigen 2); TC0600003307.mm.1 (Dusp16, dual specificity phosphatase 16, transcript variant B1, mRNA, transcript variant A1, mRNA, Complex); TC0500002030.mm.1 (NonCoding); TC1600001728.mm.1 (NonCoding); TC0600001511.mm.1 (NonCoding); TC0600002021.mm.1 (NonCoding); TC0X00000175.mm.1 (Gm14505, predicted gene 14505; novel transcript); TC1100000001.mm.1 (Pisd-ps1, phosphatidylserine decarboxylase, pseudogene 1); TC1200001873.mm.1 (NonCoding); TC0100000272.mm.1 (NonCoding); TC0100001235.mm.1 (NonCoding); TC0600002550.mm.1 (Hk2, hexokinase 2, Complex); TC1100004116.mm.1 (NonCoding); TC0900002228.mm.1 (NonCoding); TC1000001588.mm.1 (NonCoding); TC1000000942.mm.1 (NonCoding);

TC1000000999.mm.1 (NonCoding); TC0100002317.mm.1 (NonCoding); TC1000000633.mm.1 (NonCoding); TC0400001091.mm.1 (Ppap2b, phosphatidic acid phosphatase type 2B, Complex); TC0900002410.mm.1 (NonCoding); TC1200002096.mm.1 (NonCoding); TC0200001717.mm.1 (NonCoding); TC1300001090.mm.1 (NonCoding); TC0400002789.mm.1 (Wdr31, WD repeat domain 31, Complex); TC0500000340.mm.1 (NonCoding); TC0300002013.mm.1 (NonCoding); TC1200001645.mm.1 (NonCoding); TC0200003875.mm.1 (n-R5s200, nuclear encoded rRNA 5S 200, NonCoding); TCUn_JH584304000000005.mm.1 (Pisd-ps3, phosphatidylserine decarboxylase, pseudogene 3, Complex); TC0800000685.mm.1 (NonCoding); TC1300002371.mm.1 (NonCoding); TC0300000072.mm.1 (NonCoding); TC0600001278.mm.1 (Gm17482, predicted gene, 17482). Ingenuity Pathway Analysis (IPA) was used to do pathway analysis and identify activated IPA canonical pathways that may have implications in retinal regeneration. Majority of activated pathways are associated with visual system development, function, cellular proliferation, differentiation, maintenance as well as cell signaling pathways (B). Interconnectivity of various inflammatory pathways is illustrated (**C**).). Red denotes decreased gene expression and green denotes increased gene expression.

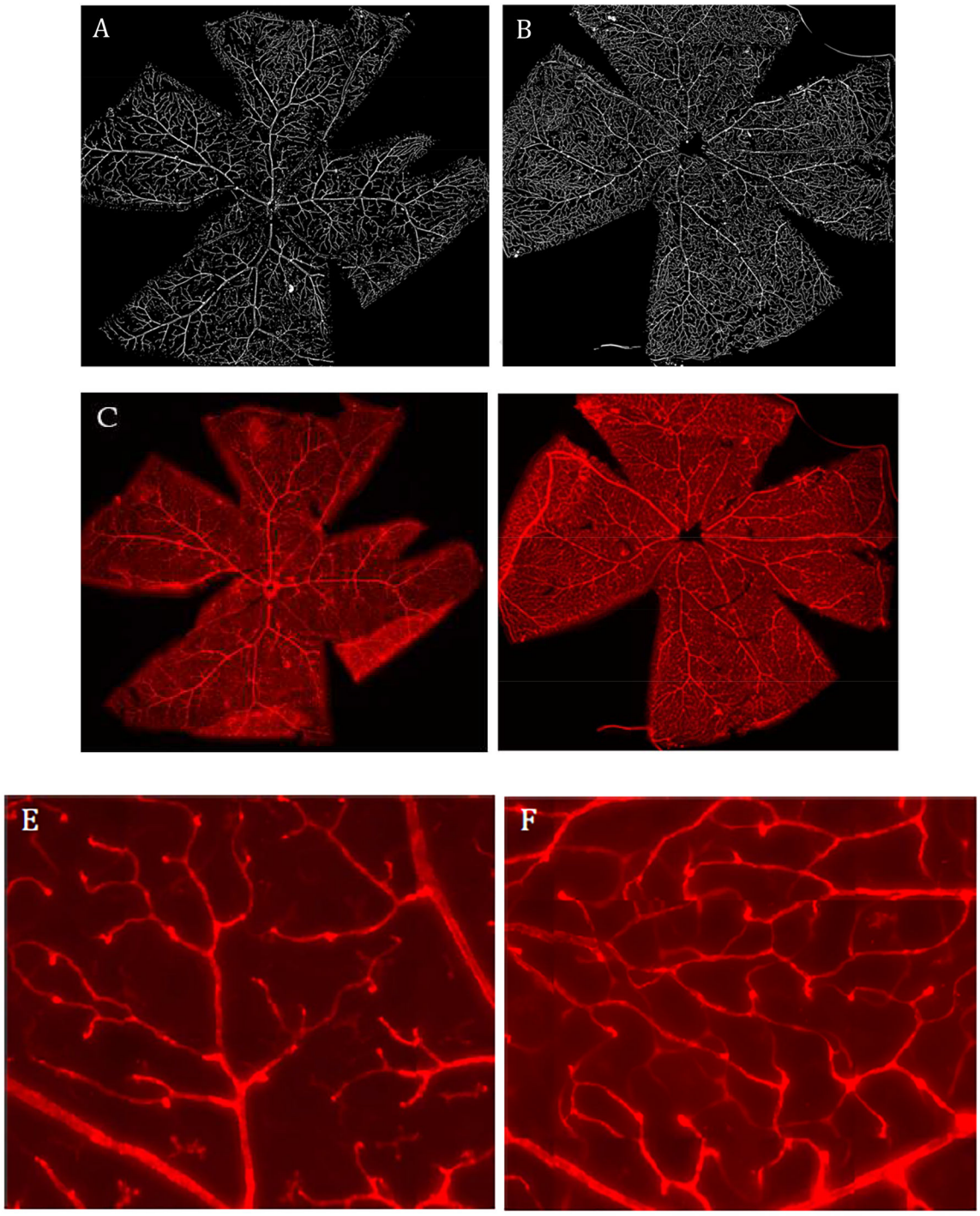

Figure 5.

Retinal vascular images on flat-mount preparation of murine retina. **(Top)** Skeletonized (binary) rendition created by Image J software Vessel Analysis plugin of the corresponding murine retinal flat-mount stained with Isolectin-GS-IB4 **(Middle). (Bottom)** High magnification images of retinal vasculature of the murine retina flat-mount. (**A, C, E**) PBS-

injected eye. (**B, D, F**) CD34+ cell-injected eye shows overall denser vascular pattern when compared with the PBS-injected eye.